accepted for publication in the Astronomical Journal

The 1000 Brightest HIPASS Galaxies: Newly Cataloged Galaxies

E. Ryan-Weber[1,2], B. S. Koribalski[2], L. Staveley-Smith[2], H. Jerjen[3], R. C. Kraan-Korteweg[4], S. D. Ryder[5], D. G. Barnes[6], W. J. G. de Blok[2], V. A. Kilborn[7,1], R. Bhathal[8], P. J. Boyce[9], M. J. Disney[10], M. J. Drinkwater[1], R. D. Ekers[2], K. C. Freeman[3], B. K. Gibson[6], A. J. Green[11], R. F. Haynes[2], P. A. Henning[12], S. Juraszek[11], M. J. Kesteven[2], P. M. Knezek[13], S. Mader[2], M. Marquarding[2], M. Meyer[1], R. F. Minchin[10], J. R. Mould[13,3], J. O'Brien[3], T. Oosterloo[14], R. M. Price[12,2], M. E. Putman[15], E. M. Sadler[11], A. Schröder[16], I. M. Stewart[16,2], F. Stootman[8], M. Waugh[1], R. L. Webster[1], A. E. Wright[2], and M. A. Zwaan[1]

[1]School of Physics, University of Melbourne, VIC 3010, Australia.

[2]Australia Telescope National Facility, CSIRO, P.O. Box 76, Epping, NSW 1710, Australia.

[3]Research School of Astronomy & Astrophysics, Mount Stromlo Observatory, Cotter Road, Weston, ACT 2611, Australia.

[4]Departamento de Astronomía, Universidad de Guanajuato, Apartado Postal 144, Guanajuato, Gto 36000, Mexico.

[5]Anglo-Australian Observatory, P.O. Box 296, Epping, NSW 1710, Australia.

[6]Centre for Astrophysics and Supercomputing, Swinburne University of Technology, P.O. Box 218, Hawthorn, VIC 3122, Australia.

[7]Jodrell Bank Observatory, University of Manchester, Macclesfield, Cheshire, SK11 9DL, U.K.

[8]Department of Physics, University of Western Sydney Macarthur, P.O. Box 555, Campbelltown, NSW 2560, Australia.

[9]Department of Physics, University of Bristol, Tyndall Ave, Bristol BS8 1TL, U.K.

[10]Department of Physics & Astronomy, University of Wales, Cardiff, P.O. Box 913, Cardiff CF2 3YB, U.K.

[11]School of Physics, University of Sydney, NSW 2006, Australia.

[12]Institute for Astrophysics, University of New Mexico, 800 Yale Blvd, NE, Albuquerque, NM 87131, USA.

[13]WIYN, Inc. 950 North Cherry Avenue, Tucson, AZ, USA.

[14]ASTRON, P.O. Box 2, 7990 AA Dwingeloo, The Netherlands.

[15]CASA, University of Colorado, Boulder, CO 80309-0389, USA.

[16]Department of Physics & Astronomy, University of Leicester, Leicester LE1 7RH, U.K.

ABSTRACT

The H I Parkes[1] All-Sky Survey (HIPASS) is a blind 21-cm survey for extragalactic neutral hydrogen, covering the whole southern sky. The HIPASS Bright Galaxy Catalog (BGC; Koribalski et al. 2002) is a subset of HIPASS and contains the 1000 H I-brightest (peak flux density) galaxies. Here we present the 138 HIPASS BGC galaxies, which had no redshift measured prior to the Parkes multibeam H I surveys. Of the 138 galaxies, 87 are newly cataloged. Newly cataloged is defined as no optical (or infrared) counterpart in the NASA/IPAC Extragalactic Database. Using the Digitized Sky Survey we identify optical counterparts for almost half of the newly cataloged galaxies, which are typically of irregular or magellanic morphological type. Several H I sources appear to be associated with compact groups or pairs of galaxies rather than an individual galaxy. The majority (57) of the newly cataloged galaxies lie within ten degrees of the Galactic Plane and are missing from optical surveys due to confusion with stars or dust extinction. This sample also includes newly cataloged galaxies first discovered in the H I shallow survey of the Zone-of-Avoidance (Henning et al. 2000). The other 30 newly cataloged galaxies escaped detection due to their low surface brightness or optical compactness. Only one of these, HIPASS J0546–68, has no obvious optical counterpart as it is obscured by the Large Magellanic Cloud. We find that the newly cataloged galaxies with $|b| > 10^\circ$ are generally lower in H I mass and narrower in velocity width compared with the total HIPASS BGC. In contrast, newly cataloged galaxies behind the Milky Way are found to be statistically similar to the entire HIPASS BGC. In addition to these galaxies, the HIPASS BGC contains four previously unknown H I clouds.

Subject headings: surveys — galaxies: distances and redshifts, fundamental parameters, kinematics and dynamics — radio emission lines

1. Introduction

The 21-cm line of neutral hydrogen (H I) is unique as it can probe regions of the sky where no stars have (yet) formed (see Schneider 1996). Within individual galaxies, H I is frequently found well outside the optical radius (e.g. Meurer et al. 1996; Salpeter &

[1]The Parkes telescope is part of the Australia Telescope which is funded by the Commonwealth of Australia for operation as a National Facility managed by CSIRO.

Hoffman 1996), and many tidal tails or bridges between galaxies are only detected in H I (see e.g. Koribalski 1996; Ryder et al. 2001). Until now, the majority of H I observations were made of objects that had first been identified in the optical (or lately the infrared), thus imposing H I selection effects on top of already existing optical selection effects. Important H I structures like the Leo ring (Schneider 1989) and the Virgo cloud (Giovanelli & Haynes 1989) were discovered by accident and indicate the enormous potential for discovery in an untargeted H I survey.

The sky has been extensively surveyed for galaxies at optical wavelengths (e.g. Lauberts 1982) but severe limitations remain, mainly due to the foreground extinction of the Milky Way (which affects ∼25% of the sky, see e.g. Kraan-Korteweg & Lahav 2000). In many optical catalogs, including the input catalogs for optical redshift surveys, low-surface brightness (LSB) galaxies are easily missed and galaxies with diameters less than $\sim 1'$ are often misclassified as stars. For example, all objects with brightness less than 1.15 times the sky and objects classified as stars were excluded from the input catalog of the Las Campanas Redshift Survey (Shectman et al. 1996). To supplement the galaxy catalogs, targeted searches for LSB galaxies (Schneider et al. 1990, 1992; Impey et al. 1996, 2001; Morshidi-Esslinger et al. 1999; Cabanela & Dickey 2000) and dwarf galaxies (Karachentseva & Karachentsev 1998; Drinkwater et al. 1999; Drinkwater et al. 2000) as well as deep optical searches for galaxies behind the southern Milky Way (Woudt & Kraan-Korteweg 2001) are being carried out. In the infrared less than 10% of the sky is affected by foreground extinction, surveys like the Two Micron All Sky Survey (2MASS, Jarrett et al. 2000) and the Deep Near-Infrared Survey of the southern sky (DENIS, Epchtein et al. 1997) are now cataloging large numbers of galaxies.

In contrast H I emission is *not* affected by extinction and enables us to identify many previously hidden galaxies. In addition, H I can easily be detected in LSB and late-type dwarf galaxies which are generally gas-rich (Impey & Bothun 1997). H I surveys complement optical galaxy catalogs and substantially improve the census of galaxies and measurement of the H I content of the local Universe. H I surveys also clarify voids by placing reliable upper limits on the mass of objects in these regions. Furthermore, there are some components of galaxies that have so far only been discovered in H I, e.g. high-velocity clouds (Putman et al. 2002), tidal H I clouds (e.g., HIPASS J0731–69, Ryder et al. 2001) and other nearby H I clouds (see e.g. Kilborn et al. 2000). Elliptical galaxies, which are typically H I-poor, are the main component missing from H I surveys (see e.g. Sanders, 1980; Knapp, Turner & Cunniffe, 1985)

The current view of the large-scale structure in the Local Universe, with its filaments and voids, is based almost entirely on optical observations of high-luminosity galaxies. This view

is highly selective and it will be interesting to see how large-scale surveys for extragalactic neutral hydrogen affect the current picture. Until recently, the Arecibo Dual-Beam Survey (ADBS) and the deeper Arecibo H I Strip Survey (AHISS) were the largest blind 21-cm surveys, covering areas of 430 and 65 deg^2 respectively. Rosenberg & Schneider (ADBS, 2000) detected 265 galaxies, of which 81 were uncataloged, whereas Zwaan et al. (AHISS, 1997; see also Zwaan 2000) detected 66 galaxies, half of which were uncataloged. With the advent of a 21-cm multibeam system at the 64-m Parkes telescope (see Staveley-Smith et al. 1996) as well as new observing and data reduction software (Barnes et al. 2001), much larger and deeper surveys are now possible. The H I Parkes All-Sky Survey (HIPASS, see e.g. Koribalski 2002) is the largest 21-cm survey for neutral hydrogen to date, covering the whole southern sky. With these surveys, extragalactic H I astronomy no longer depends entirely on observations at other wavelengths.

There is a large potential for detecting invisible H I clouds and uncataloged galaxies with unusual properties in HIPASS. We expect to find many uncataloged galaxies, either hidden behind the Milky Way with H I properties similar to the overall galaxy population or missed due to optical/infrared selection criteria. The former are important for the completion of our picture of the local large-scale structure as they bridge previously known structures that are optically intercepted by the Galactic Plane (e.g. Henning et al. 2000; Sharpe et al. 2001). The latter are equally important to enhance the completeness of galaxy catalogs across all morphological types.

Subsets of HIPASS within particular regions of the sky have already been analysed. In each of these regions uncataloged galaxies were discovered, many of which are also in our sample. Five uncataloged galaxies have been found in the Centaurus A group (Banks et al. 1999). The South Celestial Cap (SCC) region of the sky ($\delta < -62°$) has been studied extensively by Kilborn et al. (2002; see also Kilborn 2001), who found 114 uncataloged galaxies (out of 536 galaxies in total). Banks et al. (1999) and Kilborn et al. (2002) searched the HIPASS data to full sensitivity, so only some of their galaxies will appear in the HIPASS Bright Galaxy Catalog (Koribalski et al. 2002). On-going analysis of the full-sensitivity HIPASS data over the total survey area is expected to reveal many more uncataloged galaxies. Henning et al. (2000) searched the H I Zone-of-Avoidance shallow survey (HIZSS; $212° \leq l \leq 36°, |b| \leq 5°$) and found 110 H I sources, 67 of which had no published optical counterpart (see also Staveley-Smith et al. 1998). An H I survey of the Great Attractor region ($l = 300°$ to $332°$, $|b| < 5°$) by Staveley-Smith et al. (2000) has so far revealed 305 galaxies, most of which were previously unknown (see also Juraszek et al. 2000). Complete analysis of deep Zone-of-Avoidance H I data is under way (Staveley-Smith et al., in prep.).

The H I properties of all 1000 galaxies in the HIPASS Bright Galaxy Catalog are presented by Koribalski et al. (2002). The optical properties of all previously catalogued galaxies in the HIPASS BGC are analysed by Jerjen et al. (2002). And the H I mass function for the HIPASS BGC will be discussed by Zwaan et al. (2002). Here we present the H I properties of 138 galaxies from the HIPASS BGC without velocity measurements prior to the Parkes multibeam surveys; 87 of these galaxies are newly cataloged – that is they do not have a cataloged optical (or infrared) counterpart listed in the NASA/IPAC Extragalactic Database (NED). The number distribution of the BGC galaxies presented in this paper are summarised in Table 1. In Section 2 we briefly describe the observations and the HIPASS BGC selection criteria as well as the method for optical (and infrared) identifications. In Section 3 we compare the H I properties of newly cataloged galaxies with low and high absolute Galactic latitudes. Section 4 contains the conclusions. A short description of all the newly cataloged galaxies with identified optical counterparts is given in the Appendix.

2. Observations & Selection Criteria

The H I Parkes All-Sky Survey (HIPASS) was conducted from 1997 to 2000 with the multibeam system on the 64-m Parkes radio telescope; it covers the whole southern sky in the velocity range from –1200 to 12700 km s^{-1}. For an overview of the survey parameters as well as data calibration and imaging techniques see Staveley-Smith et al. (1996) and Barnes et al. (2001). The HIPASS Bright Galaxy Catalog (BGC, Koribalski et al. 2002) is a subset of HIPASS and contains the 1000 H I-brightest sources in the southern sky ($\delta < 0°$) based on their peak flux density ($S_{peak} \gtrsim 116$ mJy). Although the total flux density of a galaxy (F_{HI}), which relates directly to its H I mass, is a more useful physical measurement, the peak flux density cutoff was applied as the observations were made in the spectral domain. Consequently this is not a total flux density limited sample.

The HIPASS BGC selection criteria are briefly described below. The following velocity ranges were searched for H I signals: $-1200 < v < -350$ km s^{-1} and $350 < v < 8000$ km s^{-1}, i.e. omitting the range $|v| < 350$ km s^{-1} where confusion with high-velocity clouds (see Putman et al. 2002) makes it difficult to find galaxies.[2] Known galaxies with $|v| < 350$ km s^{-1} as well as HIZSS galaxies (Henning et al. 2000) were added to the sample. The resulting cutoff, after fitting the H I parameters and selecting the 1000 brightest H I sources, is $S_{peak} \gtrsim 116$ mJy. This corresponds to a typical minimum detection level of 9σ.

[2]Throughout the paper, the quoted velocities are in the optical convention ($v = cz$) and heliocentric velocity frame.

The galaxy finding process, selection criteria, fitting and analysis of the H I parameters and identification of cataloged optical counterparts are described by Koribalski et al. (2002). The FWHM of the gridded HIPASS beam is 15.′5 and the velocity resolution is 18 km s^{-1}. The search for optical (and infrared) counterparts was conducted using NED. We define newly cataloged as any galaxy without an optical (or infrared) counterpart in NED. For all newly cataloged galaxies, images from the Digitized Sky Survey (DSS I & II) were searched for optical counterparts within an area of $15' \times 15'$ centered on the H I position. Fig. 1 shows the separations between H I and optical positions. Galaxy positions from HIPASS are accurate to within a few arcminutes, depending on the H I peak flux density and source extent (Barnes et al. 2001). In addition, offsets from the optical position can occur intrinsicly due to multiple optical counterparts, asymmetries or warping of the H I. After completion of the identifications with NED late in the year 2000, references to a small number of the newly cataloged galaxies appeared in the literature, these are noted in Table 2. Since NED is a dynamic compilation, the counterparts presented here are valid for NED 2002, March 15th. Some galaxies may also be present in other catalogs not included in NED (e.g. The APM Sky Catalogue), these have not been searched.

3. Results and Discussion

There are 138 galaxies without velocity measurements prior to the Parkes multibeam H I surveys in the HIPASS BGC. Their distribution on the sky (Fig. 2) compared to all known HIPASS BGC galaxies, reveals — not surprisingly — most lie near the Galactic Plane. This is emphasised in the Galactic latitude histogram (Fig. 3). In the following we concentrate our study on the 87 newly cataloged galaxies listed in Table 2. For the analysis we divide the newly cataloged galaxies into two samples: there are 57 galaxies with $|b| < 10^\circ$ (see § 3.1) and 30 galaxies with $|b| > 10^\circ$ (see § 3.2). We discuss the H I properties of the two samples and derive optical properties where possible. In § 3.3 we briefly discuss the remaining 51 known galaxies without previous velocity measurements. A short description of the newly cataloged galaxies for which we have identified optical counterparts is given in the Appendix. Although H I parameters of the same HIPASS galaxies may vary slightly between catalogs, depending on the chosen fitting parameters, the original HIPASS name of each source is maintained for consistency and cross-identification purposes.

Table 2 lists the H I properties of the 87 newly cataloged galaxies. Optical properties are given for those H I sources with one or more counterparts in the DSS . The columns are as follows:
Column 1 — HIPASS Name;

Column 2 & 3 — HIPASS position;
Column 4 & 5 — Galactic longitude, l, and latitude, b, in degrees;
Column 6 — Heliocentric H I systemic velocity, $v_{\rm sys}$, in $\rm km\,s^{-1}$;
Column 7 — 50% H I velocity width, w_{50}, in $\rm km\,s^{-1}$;
Column 8 — 20% H I velocity width, w_{20}, in $\rm km\,s^{-1}$;
Column 9 — Logarithm of the H I mass, $\rm M_{HI}$, in $\rm M_\odot$;
Column 10 & 11 — Position of the optical counterpart(s);
Column 12 — Morphological type within the extended Hubble classification system (estimated by eye from the DSS);
Column 13 — References.

We adopt a uniform percentage error of 10% on all integrated H I flux densities. This is an empirical estimate based on a comparison of integrated H I flux densities of 620 galaxies in the LEDA database (see Koribalski et al. 2002). To calculate the H I mass, recessional velocities were corrected for the motion of the Sun around the Galaxy and the motion of the Galaxy in the Local Group. The correction used is the IAU convention, $v_{\rm LG} = v_{\rm sys} + 300\ \sin(l)\ \cos(b)$. The H I mass of each galaxy is then calculated using $\rm M_{HI} = 2.356 \times 10^5\ D^2\ F_{HI}$ (Giovanelli & Haynes 1988), where $\rm F_{HI}$ is the integrated H I flux density in $\rm Jy\,beam^{-1}\,km\,s^{-1}$ and $D = v_{\rm LG}\,/\,\rm H_o$ is the distance in Mpc. We adopt a Hubble constant of $\rm H_o = 75\ km\,s^{-1}\,Mpc^{-1}$.

The HIPASS BGC also contains four H I sources, which are most likely H I clouds; no obvious optical counterparts have been identified for these sources, and investigations as to their nature are under way. Three H I clouds are possibly Magellanic debris (Koribalski et al., in prep.) and lie within $\sim$10° of each other, all with heliocentric velocities $\sim$400 $\rm km\,s^{-1}$: HIZOA J1616–55 (Staveley-Smith et al. 1998), HIPASS J1712–64 (Kilborn et al. 2000), and HIPASS J1718–59 (Koribalski 2001). The fourth cloud, HIPASS J0731–69 (Ryder et al. 2001), is believed to be a tidal H I cloud associated with the NGC 2442 galaxy group.

3.1. Newly Cataloged galaxies with low absolute Galactic latitudes ($|b| < 10°$)

There are 57 newly cataloged galaxies with absolute Galactic latitudes smaller than ten degrees. As expected, very few (14) of these have counterparts in the Digitized Sky Survey; their optical morphologies range from (Sc) spirals to magellanic irregular (Im) galaxies. These galaxies are mainly absent from optical catalogs because of Galactic foreground extinction. As expected, their H I properties are similar to the known galaxies in the HIPASS BGC. We expect a small number ($\sim$3% – since we find 30 newly cataloged BGC galaxies with $|b| > 10°$ out of 1000) of these to suffer from both intrinsic low surface brightness and

Galactic extinction. Indeed, the morphological type of some newly cataloged galaxies with $|b| < 10^\circ$ is indicative of this (see Appendix and Table 2). Spectra of these 57 galaxies are given in Figure 14.

Thirty seven of the newly cataloged HIPASS BGC galaxies have $|b| < 5^\circ$ (see Fig 3). The H I Zone-of Avoidance shallow survey (Henning et al. 2000), which is independent from HIPASS, contains 32 of these galaxies, plus HIZSS 019 at $b = -5\overset{\circ}{.}5$. The five additional galaxies are HIPASS J1441–62, J1526–51, J1758–31, J1812–21, and J1851–09. These were missed in the HIZSS because of their relatively narrow H I profiles ($w_{50} < 100$ km s^{-1}). We identify optical counterparts for only seven of the galaxies with Galactic latitudes of $|b| < 5^\circ$ (see Table 2). Using DENIS, Schröder et al. (1999, 2002) identified at least 14 near-infrared counterparts.

In some cases, optical or infrared counterparts can be seen despite very high foreground extinction (Schlegel, Finkbeiner, & Davis 1998). An example is HIPASS J0730–22 (HIZSS 012; $b = -1\overset{\circ}{.}9$, $A_B = 7.8$ mag), a spectacular edge-on galaxy with a systemic velocity of 779 km s^{-1} ($v_{LG} = 528$ km s^{-1}) and a diameter of $\sim 10'$ (20 kpc). We estimated a total dynamical mass within this diameter of $\sim 5 \times 10^{10}$ $M_\odot$.

HIPASS J1532–56 (HIZSS 097, HIZOA J1532–56; $b = -0\overset{\circ}{.}1$) is the only extended (for definition, see Koribalski et al. 2002) source in the newly cataloged BGC sample. ATCA H I observations by Staveley-Smith et al. (1998) show it to be an interacting system.

3.2. Newly Cataloged galaxies at high absolute Galactic latitudes ($|b| > 10^\circ$)

There are 30 newly cataloged galaxies with absolute Galactic latitudes larger than ten degrees. All but one of these galaxies have a potential optical counterpart. Twenty-five have a single optical counterpart and four have two or more possible counterparts. The one galaxy without a possible optical counterpart is HIPASS J0546–68, which lies behind the Large Magellanic Cloud (LMC). The field is too obscured to identify an optical counterpart in this case (see Dutra et al. 2001).

Optical images and H I spectra of 25 newly cataloged galaxies with a single optical counterpart are shown in Fig. 4 and Fig. 5, respectively. The four sources with two or more potential optical counterparts, HIPASS J0605–14, J1225–06, J1244–08 and J1647–00, are displayed separately in Figs. 6, 7, 8 & 9).

Galaxies have been morphologically classified within the extended Hubble system set out for giants by Hubble (1926; 1927) and for dwarfs by Sandage & Binggeli (1984). The optical

morphology of these galaxies (see Table 2) is dominated by magellanic spiral and irregular galaxies as well as Blue Compact Dwarf (BCD) galaxies. In terms of surface brightness we find most galaxies in two distinct groups: very compact sources of high surface brightness (e.g., HIPASS J0617–17 and J2200–56) and extended sources of low surface brightness (e.g., HIPASS J1106–14 and J1255–03). There are also a few galaxies that have both signatures, a bright core and a low surface brightness disk (e.g. HIPASS J1415-04A and J1424–16B). We conclude that the newly cataloged galaxies with $|b| > 10^\circ$ are mostly absent from optical catalogs because of their small optical diameters or low surface brightness. The velocity distribution (Fig. 10) shows that newly cataloged galaxies at high absolute Galactic latitudes follow the same general trend as all the newly cataloged galaxies, which is similar to that of the whole HIPASS BGC (Koribalski et al. 2002). But their H I mass distribution (see Fig. 11) is significantly shifted towards lower values. The median of the mass distribution shifts from $\log(M_{HI}/M_\odot) = 9.4$ for newly cataloged galaxies with $|b| < 10^\circ$ to $\log(M_{HI}/M_\odot) = 8.7$ for newly cataloged galaxies with $|b| > 10^\circ$. A Kolmogorov-Smirnov test was performed and the distribution of H I masses from the two data sets very found to differ at the 99.6% level. The median H I mass of the entire HIPASS BGC is $\log(M_{HI}/M_\odot) = 9.5$, similar to that of the newly cataloged galaxies with $|b| < 10^\circ$.

In Fig. 12 we explore the H I profile shapes of the newly cataloged galaxies by comparing the measured 50% and 20% velocity widths. We find that most of the newly cataloged galaxies at high absolute Galactic latitudes have narrow H I profiles (mean $w_{50} = 64$ km s^{-1}). This value stands in sharp contrast to the equivalent parameter derived for newly cataloged galaxies with $|b| < 10^\circ$ (135 km s^{-1}). A recent survey of local dwarf galaxies (Huchtmeier, Karachentsev, & Karachentseva 2001) found a mean H I line width of $w_{50} = 66$ km s^{-1} (from 98 H I detected dwarf galaxies, velocity resolution for most galaxies = 6.2 km s^{-1}), which is similar to our value for newly cataloged galaxies with $|b| > 10^\circ$. Likewise, the standard deviation of w_{50} for our sample is 38 km s^{-1} and Huchtmeier et al. (2001) find 49 km s^{-1}. Correcting for velocity resolution does not alter these results. Interestingly they find some galaxies with very narrow profiles ($w_{50} < 20$ km s^{-1}, which would not be found by HIPASS. Narrow H I velocity profiles are indicative of either face-on spiral galaxies or low-luminosity galaxies, such as dwarfs. Given that this catalog is peak flux density selected, future HIPASS catalogs can be selected by integrated flux density and can contain newly cataloged galaxies with a different distribution of profiles, including those from highly inclined spiral galaxies.

There are three galaxies, HIPASS J0403–01, J0605–14 and J1415–04A with $|b| > 10^\circ$, for which we measure $w_{20} \gtrsim 200$ km s^{-1}. The large 20% velocity width of HIPASS J0403–01 ($v_{sys} = 910$ km s^{-1}) is probably due to confusion with H I in and around NGC 1507 (= HIPASS J0404–02, $v_{sys} = 863$ km s^{-1}, see Koribalski et al. 2002). HIPASS J0605–14 is potentially associated with a small group of galaxies. And HIPASS J1415–04A is an edge-on

spiral galaxy, close to HIPASS J1415–04B.

3.3. Known galaxies with newly cataloged velocity measurements

There are 51 cataloged galaxies, in addition to the newly cataloged galaxies, with no velocity measurement prior to the Parkes multibeam H I surveys listed in Table 3. Of these, only 17 lie within 10° of the Galactic Plane.

The columns in Table 3 are as follows:
Column 1 — HIPASS Name;
Column 2 & 3 — HIPASS position;
Column 4 & 5 — Galactic longitude, l, and latitude, b, in degrees;
Column 6 — heliocentric H I systemic velocity, $v_{\rm sys}$, in km s^{-1};
Column 7 — 50% H I velocity width, w_{50}, in km s^{-1};
Column 8 — 20% H I velocity width, w_{20}, in km s^{-1};
Column 9 — Logarithm of the H I mass, $\rm M_{HI}$, in $\rm M_\odot$;
Column 10 — Galaxy name (from NED, where 'c' means the galaxy may be confused).

Four of the galaxies in Table 3 were previously only classified as infrared sources:

- HIPASS J0747–26 (= HIZSS 022) is a very faint galaxy associated with IRAS 07451–2610. VLA H I snap-shot observations have been obtained.
- HIPASS J0809–41 (= HIZSS 035) is an edge-on galaxy with a diameter of $\sim$1.′7, identified as the extended source 2MASXi J0809537–414137 and also known as IRAS 08081–4132. ATCA H I snap-shot observations have confirmed the position.
- HIPASS J1722–05 is a faint spiral galaxy associated with IRAS 17197–0538.
- HIPASS J2118–09 is a bright compact galaxy associated with 2MASXi J2118305–090151 and IRAS 21158–0914.

3.4. Follow-up Observations

Follow-up H I observations of the newly cataloged galaxies as well as galaxy pairs/groups in the HIPASS BGC are under way with the Australia Telescope Compact Array (ATCA). The aim is to obtain accurate H I positions which will be used to check the candidate optical

(and infrared) counterparts. Some examples are shown in Fig. 13 and Table 4. The table gives the ATCA H I position, the offset from the HIPASS position, the position angle of the detection and the total integrated ATCA H I flux density. The offset between the HIPASS and ATCA position is less than $2'$ for all galaxies. In most cases the integrated ATCA H I flux density is ∼10-20% lower than the HIPASS flux density. This is typical for this type of observation since an interferometer filters out the more extended, diffuse H I emission. Such observations are particularly necessary for confused galaxies where it is not clear which of the optical counterparts are associated with the H I detection. Numerous H I follow-up observations have also been obtained by Kilborn (2001) and Kilborn et al. (2002). For example, SCC detection HIPASS J1004–73, also in our sample, has been observed with the ATCA (Kilborn 2001). It has a large (∼8 kpc) symmetric disk of H I surrounding the optical counterpart (∼2 kpc). Follow-up observations with the VLA have also taken place for some galaxies, e.g. HIPASS J0700–04 (Rivers 2000). Optical spectroscopy is planned to obtain redshifts for some of the newly cataloged galaxies.

4. Conclusions

A blind H I survey such as HIPASS provides a view of the local Universe free from optical selection effects. Although the potential for detecting previously unknown H I structures is high, we do not find any invisible H I clouds not gravitationally bound to any stellar system in the HIPASS Bright Galaxy Catalog (BGC). The four indentified H I clouds are most likely associated with Magellanic debris or other visible galaxies (The NGC 2442 group in the case of J0731–69). This can place important upper limits on the contribution of H I gas, not associated with galaxies, to the local baryon density. The HIPASS BGC has improved the census of galaxies in the local Universe by detecting galaxies behind the Milky Way. Furthermore, over the whole sky, we have easily detected galaxies missed in traditional optical surveys due to low surface brightness or misclassification as stars.

There are 87 newly cataloged galaxies in the HIPASS BGC, an additional 51 galaxies had no redshift measurement prior to the Parkes H I multibeam surveys. The majority (57) of the newly cataloged galaxies lie behind the Milky Way ($|b| < 10°$) and are missing from optical catalogs due to confusion or dust extinction. Optical counterparts are found in the Digitized Sky Survey for only 14 of these galaxies. Statistically, these 57 galaxies are found to have a similar H I mass distribution and velocity widths to the entire HIPASS BGC.

All the newly cataloged galaxies with high absolute Galactic latitudes (30) have a candidate optical counterpart(s) with morphologies ranging from late-type spiral to irregular, including four with multiple optical counterparts. The exception is HIPASS J0546–68, which

lies behind the LMC and has no visible optical counterpart. The characteristic surface brightness of these galaxies is extreme, either diffuse low surface brightness or compact high surface brightness. Although these galaxies are H I-rich, they are not high in H I mass. The newly cataloged galaxies with $|b| > 10^\circ$ on average have a lower H I mass (median $\log(M_{HI}/M_\odot) = 8.7$) and narrower velocity width (mean $w_{50} = 64$ km s^{-1}) than H I selected galaxies with optically cataloged counterparts.

Acknowledgements

- We are grateful to the staff at the ATNF Parkes and Narrabri observatories for assistance with HIPASS and follow-up observations.
- This research has made use of the NASA/IPAC Extragalactic Database (NED) which is operated by the Jet Propulsion Laboratory, California Institute of Technology, under contract with the National Aeronautics and Space Administration.
- Digitized Sky Survey (DSS) material (UKST/ROE/AAO/STScI) is acknowledged.
- SuperCOMOS Sky Surveys material is also acknowledged.

Appendix

Here we provide a short description of the newly cataloged galaxies for which optical counterparts have been identified. In addition to DSS I & II we also inspected 2MASS images, where available. Morphologically classifications have been assigned within the extended Hubble system set out for giants by Hubble (1926; 1927) and for dwarfs by Sandage & Binggeli (1984). The BCDs classified below are only candidates and will need optical spectroscopy to confirm their morphology.

Newly Cataloged galaxies with low absolute Galactic latitudes ($|b| < 10^\circ$)

The LSB appearance of galaxies in this section is mostly likely due to foreground extinction. The Galactic foreground extinction in the photometric B-band, A_B, is estimated from the IRAS DIRBE maps of Schlegel et al. (1998). Note that the extinction values from the DIRBE maps are uncalibrated at $|b| < 5^\circ$ and may be unreliable.

HIPASS J0718–09 (HIZSS 006) must be a low surface brightness galaxy, as it is not easily discernible at the relatively low extinction level of A_B = 1.9 mag. There are 2 extended patches of LSB emission visible on the DSS I image which are confirmed on the DSS II(R) image; one patch of ∼2.′0×1.′5 centered on $07^h\,18^m\,20.8^s$, –09° 03′ 20.2″, and a slightly smaller one of ∼1.′0×1.′0 centered on $07^h\,18^m\,14.5^s$, –09° 02′ 59.6″. Both together might define one very extended, face-on LSB source of up to 4′. In either case the morphology is hard to determine. Type = Sd/Sm.

HIPASS J0730–22 (HIZSS 012) is an edge-on, late-type spiral galaxy with a large angular size of ∼11′ on DSS II(R), not corrected for a Galactic extinction of A_B = 7.8 mag. The infrared counterpart is 2MASXi J0730080–220105. For a detailed discussion of the H I and infrared properties of this remarkable galaxy see Hurt et al. (2000). Type = Scd/Sd.

HIPASS J0742–34 (HIZSS 019) is a nearly face-on, late-type spiral galaxy with an angular extent of ∼1.′5×1.′0 (A_B = 6.1 mag). Its infrared counterpart is 2MASXi J0742379–343827. Type = Sc/Sd.

HIPASS J0744–35 is an edge-on spiral galaxy with a distinct bulge, very clear on DSS II(R) and 2MASS images (A_B = 4.3 mag). Type = Sc.

HIPASS J0746–28 (HIZSS 021) is a nearby, irregular galaxy with an angular extent of ∼40″×20″, very clear (A_B = 4.3 mag). It is not visible on the 2MASS image. Type = Im.

HIPASS J0833–37 (HIZSS 045) is a galaxy with an angular extent of ∼25″×20″ with a bright bulge/nucleus and a small LSB envelope. It seems a bit small for the velocity (v_{sys} = 958 km s^{-1}) and the extinction (A_B = 3.78 mag) but could have an obscured LSB halo. Type = Sm? or bulge/nucleus of earlier type galaxy.

HIPASS J0904–37 is an extremely LSB, extended (1.′75×1.′5), face-on spiral dwarf galaxy. It has a bright, small bulge/nucleus and an extended LSB disk (A_B = 2.2 mag). Type = Sc/Sd.

HIPASS J0917–53 (HIZSS 053) is an edge-on, irregular galaxy with an angular extent of ∼1.′0×0.′2 (A_B = 3.6 mag). The surrounding field is very crowded with stars. Type = Sc.

HIPASS J0957–48 (HIZSS 060) is a spiral galaxy with an angular extent of ∼40″×30″ (A_B = 2.5 mag). It consists mainly of a bulge with some LSB halo around it (one star very close to the center). The morphology is difficult to classify. Type = middle to late-type spiral.

HIPASS J1430–54 is an extremely LSB face-on spiral disk with a very small possible nucleus, visible but even fainter on DSS II(R) (A_B = 2.9 mag). See also the ATCA image in Fig. 13. Type = Sc.

HIPASS J1436–53 (WKK3285) is a LSB dwarf galaxy (A_B = 3.4 mag), visible on SRC-J film, very weak on DSS I and DSS II(R), roundish, no structure. Its angular extent is 24″×17″, B = 17.7 mag. See also the ATCA image in Fig. 13 and Woudt & Kraan-Korteweg (2001). Type = Im.

HIPASS J1451-50 has a small bright nucleus with a symmetric outer envelope (A_B = 1.4). See also the ATCA image in Fig. 13. Type = Sm.

HIPASS J1522–49 (WKK4860) is a galaxy with LSB extended features, a bit clumpy on SRC-J film (A_B = 2.6 mag). It is not visible on DSS I and very weak on DSS II(R). Its angular extent is 67″×20″, see also Woudt & Kraan-Korteweg (2001). B = 16.6 mag. Type = Im.

HIPASS J1605–57 (HIZSS 101, HIZOA J1605–57, WKK5834) is a galaxy with multiple stars superimposed (A_B = 2.1 mag). See also Juraszek et al. (2000) and Woudt & Kraan-Korteweg (2001). Type = Spiral.

Newly Cataloged galaxies with high absolute Galactic latitudes ($|b| > 10°$)

HIPASS J0255–10 is a bright dwarf irregular galaxy with one or two bright H II regions, not visible on 2MASS images. Type = Im/BCD.

HIPASS J0403–01 is a LSB galaxy just East of the bright star HD 25571; it is barely visible on the 2MASS image. Its large 20% H I velocity width, w_{20} = 247 km s^{-1}, as compared to w_{50} = 96 km s^{-1} (see Fig. 5) is probably due to confusion with H I in and around the galaxy NGC 1507 (= HIPASS J0404–02, v_{sys} = 863 km s^{-1}, see Koribalski et al. 2002), located ∼20′ away. Type = Im.

HIPASS J0447–57 is another LSB galaxy just to the North-West of the bright star HD 30804. It is possibly confused. Type = Im.

HIPASS J0532–67 is an early-type spiral galaxy which lies within the boundaries of the Large Magellanic Cloud (LMC). One can recognize a prominent bulge and a low surface brightness disk component. The light distribution is too regular for a BCD (see also the 2MASS image). This galaxy was also cataloged by Kilborn et al. (2002). The H I position coincides with the infrared sources 2MASXi J0531491–672133 and IRAS 05319–6723. Type = Sa or Sb.

HIPASS J0605–14 is associated with a group of galaxies (see Fig. 6) including two possible LSB optical counterparts. The positions and types of three optical galaxies are given in

Table 2. The H I spectrum of HIPASS J0605–14 peaks quite sharply between 3000 and 3100 km s^{-1}. Additional low level emission is seen between 3100 and 3200 km s^{-1}. By integrating separately over the two velocity ranges we can associate the bright H I emission with the Im-type galaxy at the center, whereas the other two late-type galaxies are probably contained within the lower intensity H I gas envelope to the East.

HIPASS J0617–17 is a bright dwarf irregular with one bright H II region; it is not visible in the 2MASS data. Type = Im/BCD.

HIPASS J0751–55 is a spectacular very low surface brightness, irregular galaxy close to the stars CD-55 1980 and CD-55 1979. It was recently also discovered by Karachentseva & Karachentsev (2000; [KK2000] 24). Type = Sm/Im.

HIPASS J1004–73 has a small bulge with smooth transition into the disk. Some spiral structure visible in the outer regions (low surface brightness). This galaxy was also cataloged by Kilborn et al. (2002). Type = SBm.

HIPASS J1015–34 is an H I source close to ESO375-G003, but at a lower systemic velocity. The Nancay H I spectrum of ESO375-G003 shows a systemic velocity of $v_{\rm sys}$ = 3091 km s^{-1} and a velocity width of w_{20} = 191 km s^{-1} (Fouqué et al. 1990). Its H I flux density is $F_{\rm HI}$ = 4.5 Jy km s^{-1} with a peak flux of ∼30 mJy, slightly too faint for a HIPASS detection. Interestingly, the Nancay H I spectrum of ESO375-G003 also includes HIPASS J1015–34. Both sources are part of the IC 2558 galaxy group (Hopp & Materne 1985). ATCA H I observations have been obtained. There is a small high surface brightness galaxy 2′ SW of the H I center. Type = BCD.

HIPASS J1106–14 is a big LSB dwarf Irregular without prominent H II regions. It was recently discovered by Karachentsev et al. (2000; [KKS2000] 23). Type = Im.

HIPASS J1118–17 is a compact, high surface brightness galaxy of irregular shape. Type = BCD.

HIPASS J1225–06 is possibly associated with two galaxies (see Fig. 7); a high surface brightness dwarf galaxy (LCRS B122316.1–061244) and another similar galaxy at $12^{\rm h}\,25^{\rm m}\,39^{\rm s}$, $-06^\circ\,33'\,08''$. The H I profile is very narrow, suggesting a single galaxy, but there could be additional low level H I emission. Type = Im/BCD.

HIPASS J1244–08 could be associated with several galaxies (see Fig. 8), although we note that the H I spectrum shows a typical double-horn spectrum indicative of a single gas-rich galaxy. The integrated H I distribution shows a point source. The narrow profile either indicates a face-on galaxy or a slowly rotating dwarf galaxy as the main component. The full HIPASS spectrum reveals no other H I sources at this position. There are at least four

galaxies visible in the surroundings of the HIPASS position: 1) a spectacular, nearly face-on Sm galaxy at $12^{\rm h}\,45^{\rm m}\,13^{\rm s}$, –08° 21′ 31″, 2) a small, but bright edge-on galaxy, possibly in the background, 3) an edge-on Sm galaxy at $12^{\rm h}\,45^{\rm m}\,08^{\rm s}$, –08° 23′ 05″ (the infrared counterpart is 2MASXi J1245078–082305), and 4) a Im/BCD galaxy at $12^{\rm h}\,45^{\rm m}\,04^{\rm s}$, –08° 23′ 46″ (NPM1G–08.0394). The latter two show some signs of interaction. Numerous small and faint galaxies are visible to the North of this group. H I synthesis imaging is needed to study these galaxies in more detail.

HIPASS J1247–77 is a nearby irregular, LSB dwarf galaxy. An ATCA H I image has been published by Kilborn et al. (2002; their Fig. 15). HIPASS J1247–77 has the lowest H I mass ($\sim 5 \times 10^6$ $M_\odot$) among the newly cataloged galaxies in both the HIPASS BGC and the SCC sample (Kilborn et al. 2002). Type = Im.

HIPASS J1248–08 is a high surface brightness galaxy just East of the bright star HD 111310. It is also visible in the 2MASS image. The galaxy has a tiny bulge and a strong disk component. Type = late spiral, Sc.

HIPASS J1255–03 is an LSB dwarf irregular galaxy, not visible in the 2MASS image. Type = Im.

HIPASS J1258–33 is a late-type galaxy, similar to the LMC. Type = SBm.

HIPASS J1300–13B is similar to HIPASS J1258–33, except for an LSB extension of the disk to the North. Type = SBm(pec).

HIPASS J1321–31 is a dwarf irregular galaxy in the Centaurus A group. It was also discovered by Karachentseva, & Karachentsev (1998; [KK98] 195) and Banks et al. (1999). Type = Im.

HIPASS J1337–39 is also a dwarf irregular galaxy in the Centaurus A group (see Banks et al. 1999). Type = Im.

HIPASS J1415–04A is another barred late-type spiral. Its infrared counterpart is 2MASXi J1415167–042131 $v_{\rm sys} = 2899 \pm 64$ km s^{-1}, Colless et al. 2001). The diameter is approximately $1\farcm1 \times 0\farcm4$. Magnitude = 15. Type = SBd. The galaxy, HIPASS J1415-04B (see below), is a close neighbour (separation = 18′.6 or 190 kpc).

HIPASS J1415–04B is a barred Sb or Sc galaxy. It has also recently been discovered by Colless et al. (2001; 2dFGRS N145Z235, $v_{\rm sys} = 2880 \pm 89$ km s^{-1}). A second galaxy, 2dFGRS N145Z228, closer to the H I position has a much higher velocity of 16912 km s^{-1}. The diameter is approximately $0\farcm8 \times 0\farcm7$. Magnitude = 14.8. Type = SBb/c.

HIPASS J1424–16B is a late-type spiral galaxy. No bar or bulge is visible on the DSS

II(R) image, but there is some evidence for a disk. Type = Sm/Im.

HIPASS J1434–47 is a very LSB dwarf galaxy in a crowded field of stars. See also the ATCA image in Fig. 13. Type = Im.

HIPASS J1513–44 is a small galaxy. It appears too bright for an Im galaxy. Type = BCD/Im.

HIPASS J1558–10 is a dwarf galaxy. Type = Sm/BCD.

HIPASS J1647–00 is associated with a group of galaxies (see Fig. 9 at the center of the H I detection: a peculiar looking merged galaxy pair of type Sm at $16^{\rm h}\,47^{\rm m}\,59^{\rm s}$, $-00^\circ\,22'\,59''$, another Spiral at $16^{\rm h}\,48^{\rm m}\,10^{\rm s}$, $-00^\circ\,21'\,48''$ and an edge-on Sd at $16^{\rm h}\,47^{\rm m}\,59^{\rm s}$, $-00^\circ\,19'\,47''$ (see also Table 2).

HIPASS J2020–04 is a late-type spiral galaxy. Type = Sm/Im.

HIPASS J2200–56 is confused. The surrounding field shows a galaxy group or cluster in the background. The H I source is most likely associated with the galaxy APMUKS(BJ) B215715.27–564246.0 (Maddox et al. 1990) just to the West of the bright double or multiple star HD 208877. Type = BCD.

REFERENCES

Banks, G.D., et al. 1999, ApJ, 524, 612

Barnes, D.G., et al. 2001, MNRAS, 322, 486

Cabanela, J.E., & Dickey, J.M. 2000, AAS, 197, 7601

Colless, M., et al. 2001, MNRAS, 328, 1039

Drinkwater, M.J., Phillipps, S., Gregg, M.D., Parker, Q.A., Smith, R.M., Davies, J.I., Jones, J.B., & Sadler, E.M. 1999, ApJ, 511, L97

Drinkwater, M.J., Jones, J.B., Gregg, M.D., Phillipps, S. 2000, PASA, 17, 227

Dutra, C.M., Bica, E., Clariá, J. J., Piatti, A. E., & Ahumada, A.V. 2001, A&A, 371, 895

Epchtein, N., Batz, B. de, Capoani, L., et. al. 1997, Messenger, 87, 27

Fouqué, P., Bottinelli, L., Drand, N., Gouguenheim, L., Paturel, G. 1990, A&AS, 86, 473

Giovanelli, R., & Haynes, M.P. 1988, in Galactic and Extragalactic Radio Astronomy, ed. G. Verschuur & K. Kellermann, (2nd ed; New York: Springer-Verlag), 552

Giovanelli, R., & Haynes, M.P. 1989, ApJ, 346, L5

Henning, P.A., et al. 2000, AJ, 119, 2686

Hopp, U., & Materne, J. 1985, A&AS, 61, 93

Hubble, E. 1926, ApJ, 64, 321

Hubble, E. 1927, Observatory, 50, 276

Huchtmeier, W.K., Karachentsev, I.D., & Karachentseva, V.E. 2001, A&A, 377, 801

Hurt, R.L., Jarrett, T.H., Kirkpatrick, J.D., Cutri, R.M., Schneider, S.E., Skrutskie, M., & van Driel, W. 2000, AJ, 120, 1876

Impey, C.D., Sprayberry, D., Irwin, M.J., & Bothun, G.D. 1996, ApJS, 105, 209

Impey, C.D., & Bothun, G.D. 1997, ARA&A, 35, 267

Impey, C.D., Burkholder, V., & Sprayberry, D. 2001, AJ, 122, 2341

Jarrett, T.H., Chester, T., Cutri, R., Schneider, S., Skrutskie, M., & Huchra, J.P. 2000, AJ, 119, 2498

Jerjen, H., Koribalski, B.S., et al. 2002, in prep.

Juraszek, S., et al. 2000, AJ, 119, 1629

Karachentseva, V.E., & Karachentsev, I.D. 1998, A&AS, 127, 409

Karachentseva, V.E., & Karachentsev, I.D. 2000, A&AS, 146, 359

Karachentsev, I.D., Karachentseva, V.E., Suchkov, A.A., & Grebel, E.K. 2000, A&AS, 145, 415

Kilborn, V.A., et al. 2000, AJ, 120, 1342

Kilborn, V.A. 2001, PhD Thesis, University of Melbourne

Kilborn, V.A., et al. 2002, AJ, accepted

Knapp, G.R., Turner, E.L., & Cunniffe, P.E. 1985, AJ, 90, 454

Koribalski, B.S. 1996, in ASP Conf. Series 106, The Minnesota Lectures on Extragalactic Neutral Hydrogen, ed. E. D. Skillman (San Francisco: ASP), 238

Koribalski, B.S. 2001, in ASP Conf. Series, Vol. 240, Gas and Galaxy Evolution, ed. J.E. Hibbard, M.P. Rupen, & J.H. van Gorkom (San Francisco: ASP), 439

Koribalski, B.S. 2002, in ASP Conf. Series, Seeing Through the Dust, ed. R. Taylor, T. Landecker, & T. Willis (San Francisco:ASP), in press

Koribalski, B.S., Staveley-Smith, L., et al. 2002, in prep.

Kraan-Korteweg, R.C., & Lahav, O. 2000, A&ARv, 10, 211

Lauberts, A. 1982, ESO/Uppsala survey of the ESO(B) atlas

Maddox, S.J., Sutherland, W.J., Efstathiou, G., & Loveday, J. 1990, MNRAS, 243, 692

Meurer, G.R., Carignan, C., Beaulieu, S.F., & Freeman, K.C. 1996 AJ, 111, 1551

Morshidi-Esslinger, Z., Davies, J.I., & Smith, R.M. 1999, MNRAS, 304, 297

Putman, M.E., et al. 2002, AJ, 123, 873

Rivers, A.J. 2000, PhD Thesis, University of New Mexico

Rosenberg, J.L., Schneider, S.E. 2000, ApJS 130, 177

Ryder, S.D., et al. 2001, ApJ, 555, 232

Salpeter, E.E., & Hoffman, G.L. 1996, ApJ, 465, 595

Sanders, R.H. 1980, ApJ, 242, 931

Sandage, A., & Binggeli, B. 1984, AJ, 89, 919

Schlegel, D.J., Finkbeiner, D.P., & Davis, M. 1998, ApJ, 500, 525

Schneider, S.E. 1996, in ASP Conf. Series Vol. 106, The Minnesota Lectures on Extragalactic Neutral Hydrogen, ed. E. D. Skillman (San Francisco: ASP), 323

Schneider, S.E. 1989, ApJ 343, 94

Schneider, S.E., Thuan, T.X., Magri, C., & Wadiak, J.E. 1990, ApJS 72, 245

Schneider, S.E., Thuan, T.X., Mangum, J. G., & Miller, J. 1992, ApJS 81, 5

Schröder, A., Kraan-Korteweg, R.C., & Mamon, G.A. 1999, PASA 16, 42

Schröder, A., et al. 2002, in prep.

Sharpe, J., et al. 2001, MNRAS, 322, 121

Shectman, S.A., Landy, S.D., Oemler, A., Tucker, D.L., Lin, H., Kirshner, R.P., & Schechter, P.L. 1996, ApJ, 470, 172

Staveley-Smith, L., et al. 1996, PASA, 13, 243

Staveley-Smith, L., et al. 1998, AJ, 116, 2717

Staveley-Smith, L., Juraszek, S., Henning, P.A., Koribalski, B.S., & Kraan-Korteweg, R. C. 2000, in ASP Conf. Ser. Vol. 218, Mapping the Hidden Universe, ed. R. C. Kraan-Korteweg, P. Henning & H. Andernach (San Francisco: ASP), 207

Woudt, P.A., & Kraan-Korteweg, R.C. 2001, A&A, 380, 441

Zwaan, M.A., Briggs, F.H., Spayberry, D., & Sorar,E. 1997, ApJ, 490, 173

Zwaan, M.A. 2000, PhD Thesis, University of Groningen

Zwaan, M.A, Staveley-Smith, L., Koribalski, B.S. et al. 2002, in prep.

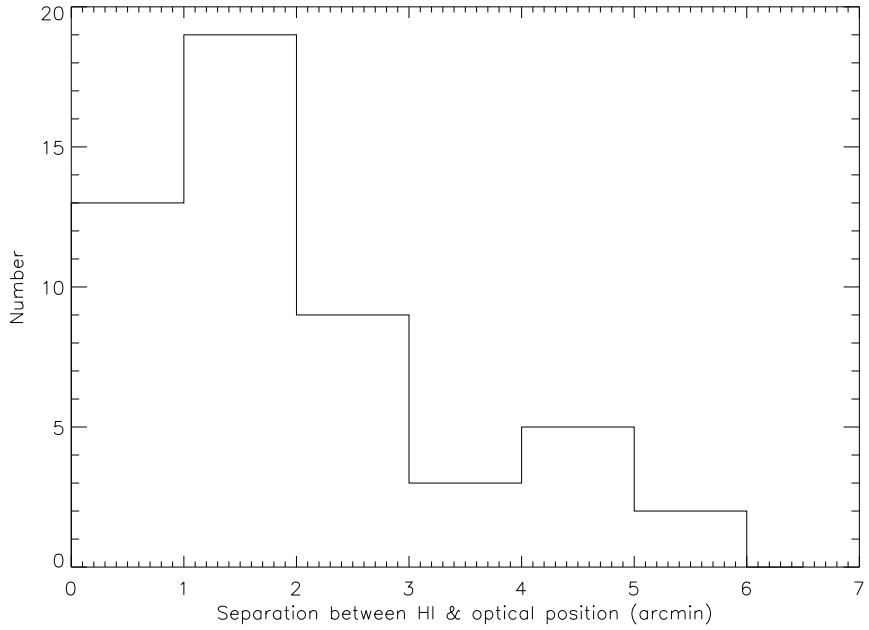

Fig. 1.— Histogram of the angular separations between HIPASS and optical position for those newly cataloged galaxies in the HIPASS Bright Galaxy Catalog for which optical counterparts are identified in the Digitized Sky Survey (see Table 2).

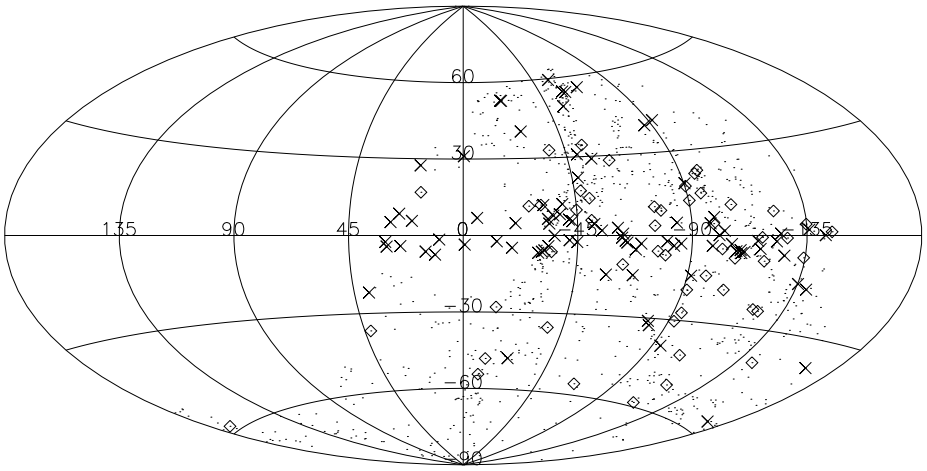

Fig. 2.— Distribution of all galaxies from the HIPASS Bright Galaxy Catalog (Koribalski et al. 2002) in Galactic coordinates. The 87 newly cataloged galaxies (×) and the 51 known galaxies with no velocity measurements prior to the Parkes multibeam H I surveys (◇) are marked.

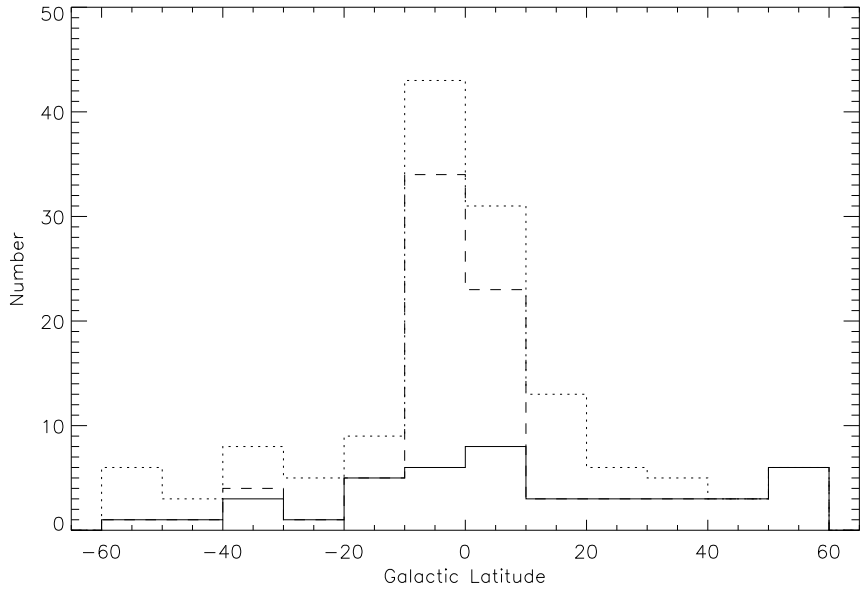

Fig. 3.— Galactic latitude histogram of the 138 HIPASS BGC galaxies with no previous velocity measurements (dotted lines). The dashed lines mark the subset of 87 newly cataloged galaxies, and the solid lines indicate the 43 newly cataloged galaxies for which we identify optical counterparts in the Digitized Sky Survey.

Fig. 4.— DSS images ($5' \times 5'$) of the 25 newly cataloged galaxies with high absolute Galactic latitudes ($|b| > 10°$) and a single candiate optical counterpart. Each DSS image is centered on the optical position.

Fig. 5.— H I spectra of the newly cataloged galaxies with high absolute Galactic latitudes ($|b| > 10°$) in the HIPASS BGC. The Figure location of each spectrum corresponds to the DSS image in Fig. 4. In addition we show the H I spectrum of the galaxy HIPASS J0546–68 (bottom left), which is obscured by the LMC.

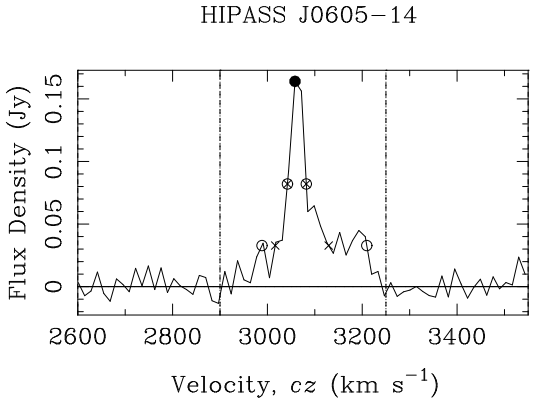

Fig. 6.— a) H I spectrum of HIPASS J0605–14. b) DSS image centered on HIPASS J0605–14. There are three potential optical counterparts. By integrating separately over the two velocity ranges (grey contours: 3000–3100 km s^{-1}; black contours: 3100–3200 km s^{-1}) we can associate the bright H I emission with the Im-type galaxy near the center, whereas the other two galaxies are probably contained within the lower intensity H I envelope to the East. The contour levels are at 60, 70, 80 and 90% of the maximum H I flux density (7.8 Jy beam^{-1} km s^{-1}).

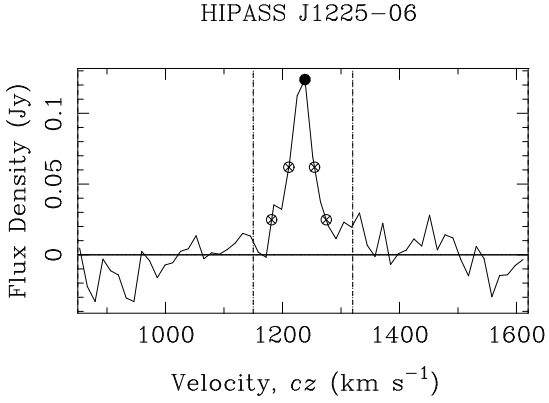

Fig. 7.— a) H I spectrum of HIPASS J1225–08. b) DSS image centered on HIPASS J1225–08. The contour levels are at 60, 70, 80 and 90% of the maximum H I flux density (5.2 Jy beam^{-1} km s^{-1}). There are two potential optical counterparts to HIPASS J1244–08 (see Table 2).

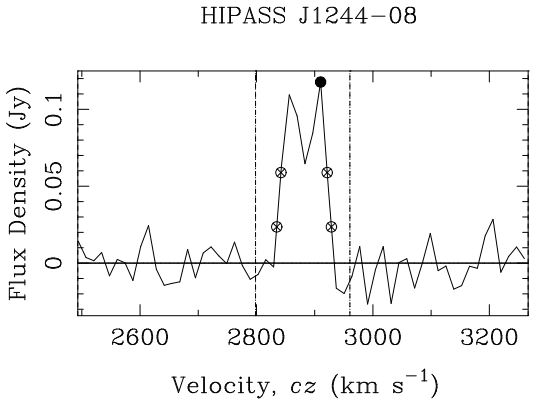

Fig. 8.— a) H I spectrum of HIPASS J1244–08. b) DSS image centered on HIPASS J1244–08. The contour levels are at 60, 70, 80 and 90% of the maximum H I flux density (5.2 Jy beam^{-1} km s^{-1}). There are at least four potential optical counterparts to HIPASS J1244–08 (see Table 2).

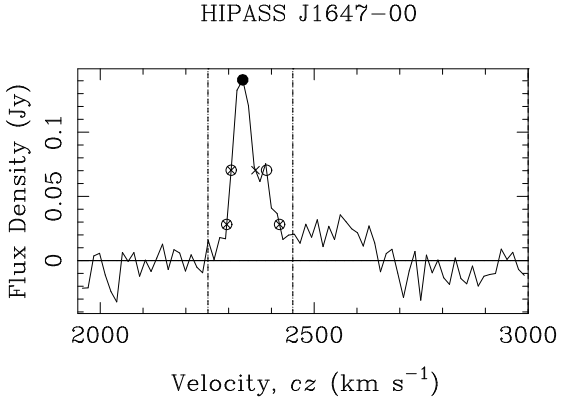

Fig. 9.— a) H I spectrum of HIPASS J1647–00. b) DSS image centered on HIPASS J1647–00. The contour levels are at 60, 70, 80 and 90% of the maximum H I flux density (10.0 Jy beam^{-1} km s^{-1}). There are three potential optical counterparts to HIPASS J1647–00 (see Table 2).

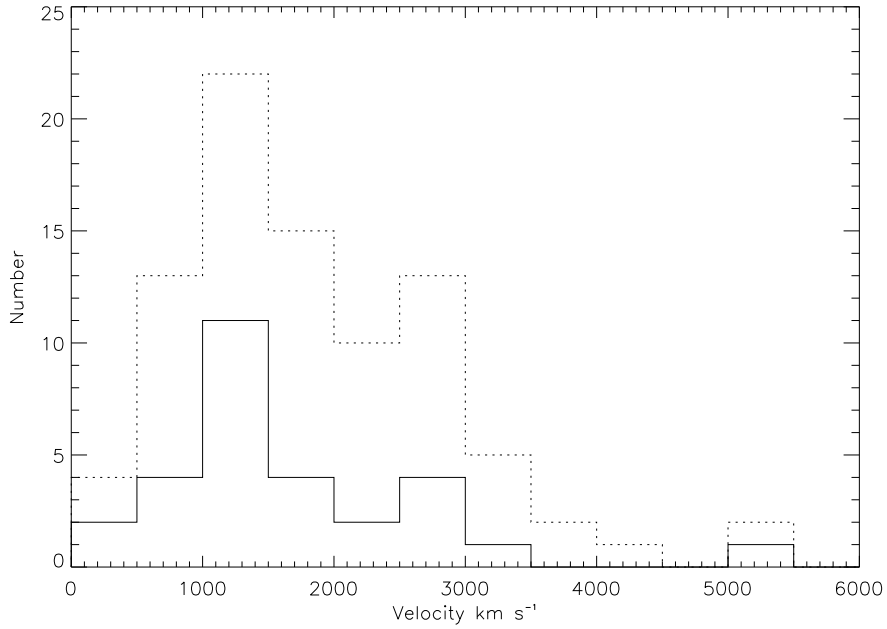

Fig. 10.— H I velocity distribution of the newly cataloged galaxies in the HIPASS Bright Galaxy Catalog (dotted histogram). The solid histogram shows the newly cataloged galaxies with $|b| > 10°$.

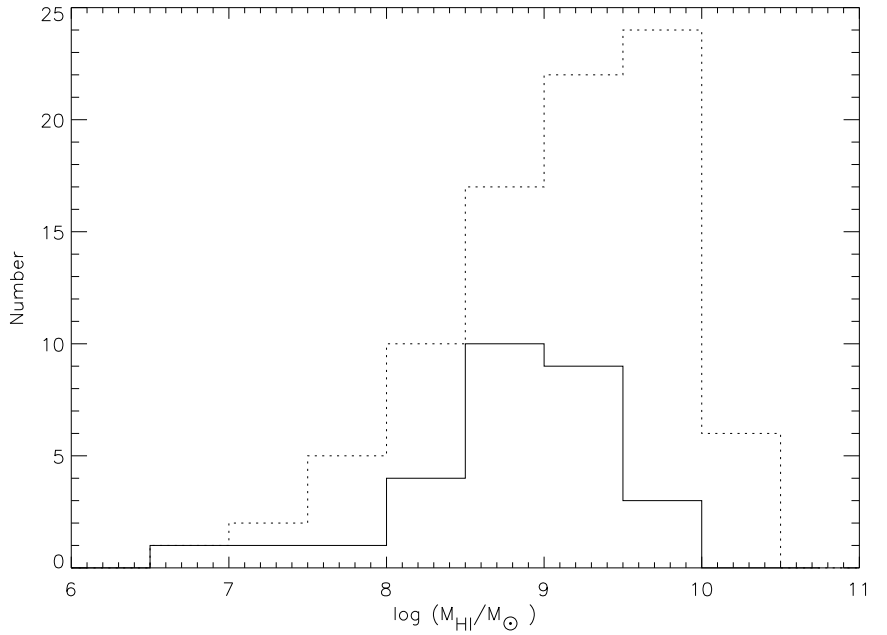

Fig. 11.— H I mass distribution of the newly cataloged galaxies in the HIPASS Bright Galaxy Catalog (dotted histogram). The solid histogram shows the newly cataloged galaxies with $|b| > 10°$.

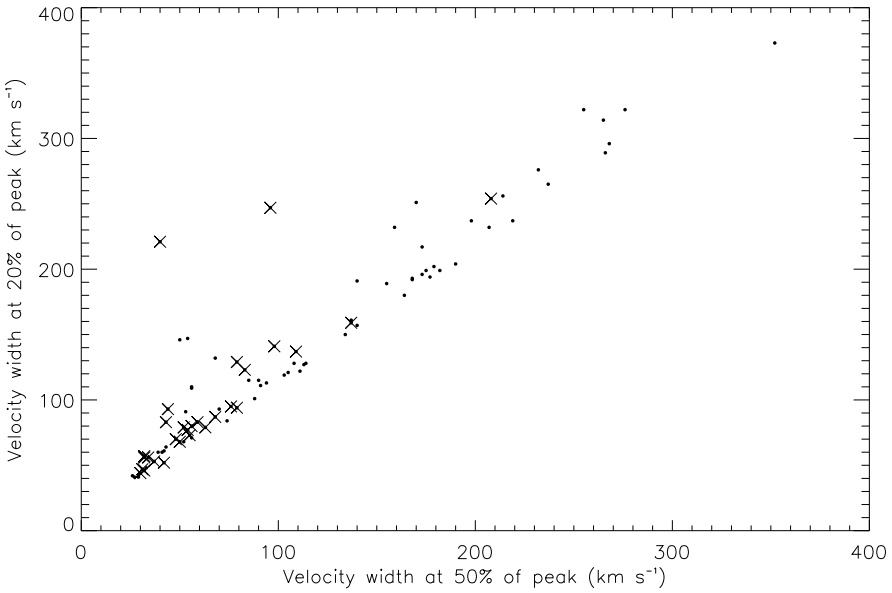

Fig. 12.— Comparison of the measured 50% H I velocity width, w_{50}, versus the 20% H I velocity width, w_{20}, for all the newly cataloged galaxies from the HIPASS Bright Galaxy Catalog. Newly Cataloged galaxies with $|b| > 10°$ are also marked (×).

Fig. 13.— ATCA H I contours overlaid on $10' \times 10'$ SuperCOSMOS fields for the galaxies HIPASS J0705–20 (b = -6°.4), J1430–54 (b = 5°.5), J1434–47 (b = 12°.1), J1436–53 (b = 6°.1), J1451–50 (b = 8°.2), and J1506–49 (b = 7°.7), arranged from top left to bottom right. These galaxies were observed on 2001 October 12, with the ATCA EW352 compact configuration (integration time ∼100 minutes each). The ATCA beam is displayed in the bottom left corner of each image. The H I contours levels are 0.5, 1, 2 then increasing in increments of 1 Jy beam^{-1} km s^{-1}.

Fig. 14.— H I spectra of the newly cataloged galaxies with low absolute Galactic latitudes ($|b| < 10°$) in the HIPASS BGC.

Fig. 14.— continued.

Category	Number $\|b\| < 10^\circ$	Number $\|b\| > 10^\circ$	Total
Newly Cataloged Galaxies (no optical or infrared counterpart in NED)			
Single counterpart	13	25	38
Confused	1	4	5
No optical seen	43	1 (Behind LMC)	44
Total	57 (including 33 HIZSS)	30	87
Galaxies with new redshifts (measured for the first time by the Parkes H I multibeam surveys)			
	17	34	51
Total			138

Table 1: Number distribution of HIPASS BGC galaxies presented in this paper.

Table 2:: H I properties of the 87 newly cataloged galaxies in the HIPASS Bright Galaxy Catalog. Optical properties are given for those H I sources with one or more counterparts in the Digitized Sky Survey (DSS).

HIPASS Name	HIPASS Properties									Optical Properties			
	α, δ(J2000)		l	b	$v_{\rm sys}$	w_{50}	w_{20}	$F_{\rm HI}$	log $M_{\rm HI}$	α, δ(J2000)		Morphology	References
	[h,m,s]	[° ′ ″]	[°]	[°]	[km s^{-1}]	[km s^{-1}]	[km s^{-1}]	[Jy km s^{-1}]	[$M_\odot$]	[h,m,s]	[° ′ ″]		
HIPASS J0255–10	02:55:27	–10:49:28	189.7	–56.6	1568	98	141	9.9	8.99	02:55:19	–10:49:14	Im/BCD	
HIPASS J0403–01	04:03:36	–01:57:26	192.7	–37.6	910	96	247	16.1	8.70	04:03:33	–01:55:45	Im	
HIPASS J0447–57	04:47:14	–57:12:35	266.2	–39.2	1248	43	83	7.6	8.52	04:47:14	–57:08:30	Im	
HIPASS J0532–67	05:31:44	–67:21:33	277.5	–32.5	1375	55	73	6.9	8.56	05:31:49	–67:21:34	Sa/Sb	J0532–67 [5], [6]
HIPASS J0546–68	05:46:21	–68:41:38	278.9	–31.0	1306	26	42	4.6	8.33				J0546–68 [5]
HIPASS J0605–14	06:05:07	–14:06:06	220.6	–16.5	3062	40	221	13.8	9.68	06:04:59	–14:06:29	Im	
										06:05:11	–14:02:10	Sm	
										06:05:21	–14:03:42	BCD	
HIPASS J0617–17	06:17:52	–17:08:50	224.8	–15.0	855	32	56	10.3	8.26	06:17:53	–17:09:04	Im/BCD	
HIPASS J0700–04	07:00:29	–04:11:37	217.7	0.1	298	70	93	26.6	7.17				HIZSS003 [3]
HIPASS J0705–20	07:05:45	–20:59:30	233.3	–6.4	766	29	41	13.2	8.19				
HIPASS J0718–09	07:18:25	–09:02:46	224.1	1.8	916	53	91	14.2	8.47	07:18:21	–09:03:20	Sd/Sm	HIZSS006 [3]
										07:18:15	–09:03:00	Sd/Sm	HIZSS006 [3]
HIPASS J0730–22	07:30:08	–22:01:27	236.8	–1.9	779	268	296	86.4	9.00	07:30:08	–22:01:06	Scd/Sd	HIZSS012 [3], [6]
HIPASS J0733–28	07:33:16	–28:41:07	243.0	–4.4	2091	54	147	10.8	9.18				HIZSS013 [3]
HIPASS J0736–19	07:36:09	–19:25:18	235.2	0.6	786	56	71	6.5	7.90				HIZSS014 [3]
HIPASS J0742–34	07:42:45	–34:38:21	249.2	–5.5	2898	232	276	33.5	9.98	07:42:38	–34:38:28	Sc/Sd	HIZSS019 [3], [6]
HIPASS J0744–35	07:44:14	–35:48:53	250.4	–5.9	2879	265	314	26.4	9.87	07:44:12	–35:48:34	Sc	
HIPASS J0746–28	07:46:21	–28:27:51	244.2	–1.8	494	85	115	22.5	7.68	07:46:16	–28:28:10	Im	HIZSS021 [3]
HIPASS J0749–35	07:49:31	–35:41:34	250.8	–4.9	2865	43	64	15.0	9.62				HIZSS025 [3]
HIPASS J0751–37	07:51:27	–37:12:56	252.4	–5.3	2804	88	101	9.6	9.41				
HIPASS J0751–55	07:51:30	–55:28:00	268.5	–14.2	1119	42	52	6.2	8.25	07:51:23	–55:27:13	Sm/Im	[KK2000] 24 [7]
HIPASS J0806–37	08:06:59	–37:43:17	254.4	–2.9	860	56	109	9.8	8.13				HIZSS033 [3]
HIPASS J0826–44	08:26:26	–44:19:28	261.9	–3.6	1023	182	199	37.1	8.91				HIZSS043 [3]
HIPASS J0833–37	08:33:56	–37:32:51	257.3	1.6	958	56	110	9.5	8.25	08:34:00	–37:32:59	Sm?	HIZSS045 [3]
HIPASS J0834–40	08:34:41	–40:08:45	259.4	0.1	2771	168	192	25.6	9.82				HIZSS046 [3]
HIPASS J0902–40	09:02:02	–40:06:37	262.7	4.2	1636	94	113	12.0	8.96				HIZSS051 [3]
HIPASS J0904–37	09:04:36	–37:22:35	261.0	6.4	1033	105	121	12.0	8.44	09:04:42	–37:22:20	Sc/Sd	
HIPASS J0917–53	09:17:36	–53:22:39	274.3	–2.9	946	173	217	18.8	8.52	09:17:31	–53:23:19	Sc	HIZSS053 [3]
HIPASS J0927–55	09:27:47	–55:59:09	277.1	–3.7	1156	140	157	34.7	9.03				HIZSS054 [3]
HIPASS J0949–56	09:49:36	–56:31:20	279.8	–2.1	1762	214	256	42.3	9.58				HIZSS059 [3]
HIPASS J0957–48	09:57:03	–48:55:41	275.9	4.6	3727	33	48	7.3	9.56	09:57:11	–48:56:30	Spiral	HIZSS060 [3]
HIPASS J1004–73	10:04:07	–73:50:50	291.9	–14.7	1246	50	68	8.0	8.51	10:04:58	–73:51:19	SBm	J1005–73 [5]
HIPASS J1015–34	10:15:47	–34:05:21	269.7	18.5	2608	32	57	5.7	9.11	10:15:38	–34:06:11	BCD	
HIPASS J1053–62	10:53:44	–62:50:43	290.0	–3.0	1836	266	289	33.5	9.53				HIZSS066 [3], [5]
HIPASS J1101–65	11:01:53	–65:45:32	292.0	–5.2	1790	42	61	8.8	8.93				J1101–65 [5]

continued

Table 2:: H I properties of the 87 newly cataloged galaxies in the HIPASS Bright Galaxy Catalog. Optical properties are given for those H I sources with one or more counterparts in the Digitized Sky Survey (DSS).

HIPASS Name	HIPASS Properties									Optical Properties			
	α, δ(J2000)		l	b	$v_{\rm sys}$	w_{50}	w_{20}	$F_{\rm HI}$	log $M_{\rm HI}$	α, δ(J2000)		Morphology	References
	[h,m,s]	[° ′ ″]	[°]	[°]	[km s^{-1}]	[km s^{-1}]	[km s^{-1}]	[Jy km s^{-1}]	[$M_\odot$]	[h,m,s]	[° ′ ″]		
HIPASS J1106–14	11:06:05	–14:22:10	268.1	41.3	1040	76	95	11.2	8.49	11:06:11	–14:24:28	Im	[KKS2000] 23 [8]
HIPASS J1118–17	11:18:03	–17:38:26	273.5	39.8	1069	52	79	10.2	8.48	11:18:03	–17:38:32	BCD	
HIPASS J1141–64	11:41:19	–64:28:41	295.5	–2.6	2025	179	202	38.6	9.70				HIZSS068 [3], [5]
HIPASS J1149–64	11:49:50	–64:00:24	296.2	–1.9	2067	255	322	45.7	9.79				HIZSS069 [3], [5]
HIPASS J1202–61	12:02:56	–61:39:03	297.2	0.7	1540	207	232	93.7	9.80				HIZSS070 [3]
HIPASS J1204–63	12:04:20	–63:11:27	297.6	–0.8	2034	168	193	29.3	9.58				HIZSS071 [3], [5]
HIPASS J1221–59	12:21:39	–59:42:21	299.2	2.9	1477	175	199	40.1	9.40				HIZSS073 [3]
HIPASS J1225–06	12:25:33	–06:31:09	291.4	55.8	1233	44	93	7.3	8.55	12:25:51	–06:29:22	Im/BCD	[9]
										12:25:39	–06:33:08	Im/BCD	
HIPASS J1244–08	12:44:59	–08:18:23	300.2	54.5	2882	79	94	7.3	9.36	12:45:13	–08:21:31	Sm	
										12:45:08	–08:23:05	Sm	[6]
										12:45:04	–08:23:46	Im/BCD	[10]
HIPASS J1247–77	12:47:26	–77:34:17	302.7	–14.7	413	32	46	4.7	6.75	12:47:34	–77:34:54	Im	[5]
HIPASS J1248–08	12:48:28	–08:01:49	301.7	54.8	1502	63	79	22.2	9.23	12:48:31	–08:02:37	Sc	
HIPASS J1255–03	12:55:16	–03:23:39	304.8	59.5	1484	34	56	8.0	8.79	12:55:11	–03:24:12	Im	
HIPASS J1258–33	12:58:43	–33:45:21	304.7	29.1	2476	59	83	7.5	9.21	12:58:36	–33:45:35	SBm	
HIPASS J1300–13B	13:00:58	–13:31:27	306.5	49.3	1309	56	80	7.0	8.59	13:01:07	–13:31:04	SBm(pec)	
HIPASS J1312–60	13:12:47	–60:52:40	305.5	1.9	2321	237	265	32.3	9.77				HIZSS076 [3]
HIPASS J1321–31	13:21:07	–31:33:03	310.3	30.9	571	31	47	5.9	7.54	13:21:08	–31:31:45	Im	[2], [KK98] 195 [11]
HIPASS J1333–58	13:33:00	–58:03:50	308.4	4.4	1476	111	122	12.4	8.90				HIZSS080 [3], [4]
HIPASS J1337–39	13:37:30	–39:52:56	312.5	22.1	492	37	53	6.6	7.36	13:37:26	–39:53:47	Im	[2]
HIPASS J1415–04A	14:15:08	–04:20:00	338.8	52.6	2740	208	254	21.4	9.81	14:15:17	–04:21:31	SBd	[6], [12]
HIPASS J1415–04B	14:15:56	–04:04:02	339.3	52.7	2730	54	77	8.0	9.38	14:15:47	–04:04:32	SBb/c	[12]
HIPASS J1424–16B	14:24:29	–16:58:58	332.7	40.5	1487	68	87	13.4	9.03	14:24:31	–16:59:15	Sm/Im	
HIPASS J1430–54	14:30:18	–54:36:23	317.0	5.5	3020	114	128	9.6	9.50	14:30:16	–54:36:22	Sc	
HIPASS J1434–47	14:34:36	–47:12:05	320.5	12.1	1512	30	44	4.8	8.55	14:34:44	–47:13:35	Im	
HIPASS J1436–53	14:36:50	–53:34:40	318.3	6.1	3016	108	128	31.2	10.02	14:36:48	–53:34:22	Im	WKK3285 [13]
HIPASS J1441–62	14:41:37	–62:44:38	315.2	–2.5	672	52	68	4.7	7.62				[5]
HIPASS J1451–50	14:51:21	–50:13:55	321.8	8.2	1275	164	180	24.8	9.09	14:51:13	-50:12:47	Sm	
HIPASS J1501–60	15:01:30	–60:44:53	318.2	–1.8	4436	134	150	14.7	10.04				HIZSS092 [3], [4]
HIPASS J1506–49	15:06:58	–49:24:47	324.4	7.7	1041	113	127	29.7	8.97				
HIPASS J1513–44	15:13:10	–44:03:10	328.1	11.8	5125	48	70	7.8	9.91	15:13:13	–44:02:00	BCD/Im	
HIPASS J1522–49	15:22:22	–49:22:09	326.6	6.4	2307	173	196	19.3	9.57	15:22:24	–49:21:29	Im	WKK4860 [13]
HIPASS J1526–51	15:26:18	–51:09:46	326.1	4.6	605	39	60	6.0	7.68				HIZOA J1526–51 [4]
HIPASS J1532–56	15:32:55	–56:08:35	324.1	–0.1	1363	68	132	64.2	9.58				[1], HIZSS097 [3], [4]
HIPASS J1558–10	15:58:27	–10:30:45	359.7	31.1	933	79	129	11.4	8.62	15:58:20	–10:32:16	Sm/BCD	
HIPASS J1605–57	16:05:19	–57:52:04	326.5	–4.1	2991	91	111	17.5	9.77	16:05:22	–57:51:43	Spiral	HIZSS101 [3], [4], [13]

continued

Table 2:: H I properties of the 87 newly cataloged galaxies in the HIPASS Bright Galaxy Catalog. Optical properties are given for those H I sources with one or more counterparts in the Digitized Sky Survey (DSS).

HIPASS Name	HIPASS Properties									Optical Properties			
	α, δ(J2000)		l	b	$v_{\rm sys}$	w_{50}	w_{20}	$F_{\rm HI}$	log $M_{\rm HI}$	α, δ(J2000)		Morphology	References
	[h,m,s]	[° ′ ″]	[°]	[°]	[km s^{-1}]	[km s^{-1}]	[km s^{-1}]	[Jy km s^{-1}]	[$M_\odot$]	[h,m,s]	[° ′ ″]		
HIPASS J1621–58	16:21:50	–58:00:06	328.0	–5.8	1404	74	84	9.4	8.79				
HIPASS J1624–42	16:24:54	–42:29:35	339.4	4.8	2232	159	232	21.5	9.61				HIZSS104 [3]
HIPASS J1629–57	16:29:58	–57:39:09	329.0	–6.3	2685	198	237	14.4	9.59				
HIPASS J1639–56	16:39:41	–56:52:35	330.4	–6.7	1468	103	119	18.9	9.14				
HIPASS J1647–00	16:47:55	–00:23:08	18.1	27.4	2347	83	123	11.3	9.45	16:47:59	–00:22:59	Sm(Gpair)	
										16:48:10	–00:21:48	Spiral	
										16:47:59	–00:19:47	Sd	
HIPASS J1705–29	17:05:26	–29:40:38	354.5	6.9	2677	177	194	19.1	9.75				
HIPASS J1711–47	17:11:35	–47:35:59	340.8	–4.8	2187	219	237	21.1	9.59				HIZSS106 [3]
HIPASS J1719–41	17:19:48	–41:18:14	346.8	–2.3	3902	276	322	27.0	10.22				HIZSS107 [3]
HIPASS J1758–31	17:58:37	–31:18:11	359.4	–3.6	3316	41	60	5.5	9.40				
HIPASS J1807–02	18:07:10	–02:49:17	25.3	8.5	1765	137	161	35.3	9.72				
HIPASS J1807–08	18:07:39	–08:36:38	20.2	5.7	3485	170	251	19.0	10.01				
HIPASS J1812–21	18:12:22	–21:34:07	9.4	–1.6	1533	50	146	11.2	9.07				
HIPASS J1824–01	18:24:58	–01:28:03	28.6	5.2	2865	352	373	31.6	10.08				
HIPASS J1838–22	18:38:36	–22:48:25	11.1	–7.5	1656	27	41	9.4	9.06				
HIPASS J1841–18	18:41:05	–18:59:54	14.8	–6.3	1671	155	189	15.7	9.30				
HIPASS J1851–09	18:51:19	–09:10:53	24.7	–4.1	5485	90	115	9.8	10.11				
HIPASS J1856–03	18:56:00	–03:10:21	30.6	–2.5	1582	190	204	21.7	9.44				HIZSS108 [3]
HIPASS J1901–04	19:01:44	–04:29:37	30.1	–4.3	1530	140	191	23.9	9.45				HIZSS109 [3]
HIPASS J2020–04	20:20:35	–04:54:16	38.9	–22.0	1387	109	137	11.9	9.09	20:20:32	–04:54:00	Sm/Im	
HIPASS J2200–56	22:00:42	–56:28:10	336.9	–47.9	1847	137	159	19.0	9.40	22:00:40	–56:28:20	BCD	[9]

Catalog and reference codes: [1] Staveley-Smith et al. (1998); [2] Banks et al. (1999); [3] HIZSS, Henning et al. (2000); [4] HIZOA, Juraszek et al. (2000); [5] HIPASS SCC, Kilborn et al. (2002); [6] 2MASXi, Jarret et al. (2000); [7] KK2000, Karachentseva & Karachentsev (2000); [8] KKS2000, Karachentsev et al. (2000); [9] APMUKS(BJ), Maddox et al. (1990); [10] NPM1G, Klemola et al. (1987); [11] KK98, Karachentseva & Karachentsev (1998); [12] 2dFGRS, Colless et al. (2001); [13] WKK, Woudt & Kraan-Korteweg (2001).

Table 3:: H I properties of the additional 51 galaxies without a previous redshift measurement in the HIPASS Bright Galaxy Catalog.

HIPASS Name	α, δ(J2000)		l	b	$v_{\rm sys}$	w_{50}	w_{20}	$F_{\rm HI}$	log $M_{\rm HI}$	NED-ID
	[h,m,s]	[° ′ ″]	[°]	[°]	[km s^{-1}]	[km s^{-1}]	[km s^{-1}]	[Jy km s^{-1}]	[$M_\odot$]	
HIPASS J0136–60	01:36:22	–60:23:41	293.1	–55.9	2221	45	64	8.9	9.20	ESO113-IG054
HIPASS J0223–04	02:23:51	–04:36:52	171.4	–58.5	2273	96	112	13.9	9.49	PGC009103
HIPASS J0310–39	03:10:01	–39:59:14	246.1	-58.7	711	30	45	4.4	7.78	ESO300-G016
HIPASS J0348–39	03:48:32	–39:26:46	243.1	–51.4	1168	29	46	4.9	8.31	ESO302-G?010
HIPASS J0430–20	04:30:53	–20:36:45	218.0	–39.8	1627	122	149	18.7	9.24	APMBGC551+05
HIPASS J0439–47	04:39:51	–47:30:14	253.7	–41.5	1368	53	80	6.8	8.58	ESO202-IG048
HIPASS J0553–59	05:53:12	–59:03:03	267.7	–30.4	1308	120	141	14.4	8.82	ESO120-G021
HIPASS J0555–29	05:55:07	–29:56:23	235.4	–24.5	3604	31	47	5.9	9.45	ESO424-G039
HIPASS J0600–31	06:00:18	–31:48:50	237.8	-24.1	1353	90	117	10.0	8.72	ESO425-G001
HIPASS J0615–57	06:15:58	–57:44:29	266.5	–27.3	577	65	96	14.1	7.76	ESO121-G020
HIPASS J0649–14	06:49:38	–14:25:08	225.6	–6.9	2802	126	147	14.5	9.61	CGMW1-0409
HIPASS J0651–44	06:51:18	–44:05:17	253.7	–18.5	4748	46	153	8.4	9.85	ESO256-G003
HIPASS J0659–01	06:59:22	–01:31:43	215.2	1.1	1733	168	188	20.2	9.31	CGMW1-0476
HIPASS J0712–28	07:12:42	–28:40:21	240.9	–8.4	881	112	128	10.9	8.25	ESO428-G004
HIPASS J0718–57	07:18:21	–57:26:59	268.5	–19.2	1148	64	84	10.9	8.53	AM0717-571
HIPASS J0725–17	07:25:55	–17:53:15	232.7	–0.8	2758	94	167	11.8	9.50	CGMW1-0877c
HIPASS J0726–09	07:26:34	–09:14:24	225.2	3.5	2438	30	55	6.2	9.11	ZOAG_G225+03
HIPASS J0735–50	07:35:18	–50:15:57	262.6	–14.0	1200	91	123	13.0	8.66	ESO208-G025
HIPASS J0741–38	07:41:30	–38:35:39	252.6	–7.7	2789	25	44	13.1	9.54	ESO311-G003
HIPASS J0747–26	07:47:02	–26:21:13	242.5	–0.6	881	141	153	45.7	8.86	IRAS07451–2610
HIPASS J0807–17	08:07:00	–17:28:46	237.3	7.9	2370	138	164	20.3	9.58	CGMW2-2253
HIPASS J0809–41	08:09:54	–41:41:03	258.0	–4.6	1995	312	337	25.7	9.49	IRAS08081–4132
HIPASS J0857–29	08:57:09	–29:09:29	253.6	10.5	1971	20	37	3.3	8.60	CGMW2-4513
HIPASS J0857–39	08:57:28	–39:16:04	261.5	4.1	978	317	349	37.0	8.86	ESO314-G?002
HIPASS J0926–60	09:26:26	–60:35:39	280.2	-7.1	2120	125	160	18.6	9.42	ESO126-G011c
HIPASS J0945–33	09:45:33	–33:48:07	264.4	14.8	2654	63	117	7.9	9.27	ESO373-IG022
HIPASS J0953–61	09:53:00	–61:30:14	283.3	-5.7	4439	48	68	7.3	9.72	RKK1733
HIPASS J0957–39	09:57:15	–39:00:10	269.7	12.4	4652	54	99	8.2	9.82	ESO316-G006
HIPASS J1003–26B	10:03:51	–26:38:33	262.6	22.8	885	77	101	9.5	8.17	ESO499-G038c
HIPASS J1005–28	10:05:33	–28:23:40	264.1	21.7	1037	100	195	18.8	8.66	ESO435-G039c
HIPASS J1013–34	10:13:07	–34:54:50	269.7	17.5	4367	43	102	9.5	9.82	ESO374-G043
HIPASS J1040–54	10:40:20	–54:32:31	284.6	3.6	2753	109	138	15.3	9.59	RKK2791/89
HIPASS J1041–48	10:41:25	–48:19:40	281.7	9.1	989	70	80	12.3	8.40	ESO214-G018c
HIPASS J1057–48	10:57:32	–48:11:02	284.1	10.5	598	67	83	104.4	8.63	ESO215-G?009
HIPASS J1126–72	11:26:15	–72:37:06	296.6	–10.8	2031	28	38	12.2	9.20	PGC035171
HIPASS J1227–34	12:27:45	–34:25:08	297.4	28.2	2922	120	196	12.9	9.59	ESO380-IG033
HIPASS J1305–28	13:05:52	–28:22:11	306.8	34.4	2282	105	170	17.8	9.51	ESO443-G061
HIPASS J1329–48	13:29:05	–48:09:57	309.4	14.2	2034	125	151	12.3	9.23	ESO220-G014
HIPASS J1338–56	13:38:10	–56:28:30	309.4	5.8	3957	312	342	25.6	10.17	PGC048178
HIPASS J1343–44	13:43:07	–44:51:10	312.5	17.1	2200	107	154	12.0	9.30	ESO270-G026
HIPASS J1403–27	14:03:31	–27:17:09	322.0	32.9	1327	117	131	12.0	8.84	ESO510-IG052
HIPASS J1409–51	14:09:05	–51:10:43	315.1	9.8	4530	132	164	14.1	10.04	ESO221-G028
HIPASS J1517–43	15:17:46	–43:29:01	329.1	11.8	5001	28	67	4.6	9.66	ESO274-G009
HIPASS J1539–41	15:39:39	–41:10:54	333.9	11.4	2390	161	181	20.8	9.65	ESO329-G?013
HIPASS J1609–60	16:09:44	–60:18:00	325.2	-6.3	3246	170	242	21.7	9.94	ESO136-G020
HIPASS J1722–05	17:22:22	–05:43:07	17.1	16.9	1625	134	191	30.1	9.57	IRAS17197–0538
HIPASS J1937–52	19:37:37	–52:00:42	346.0	–28.0	3157	206	247	23.6	9.98	IC4877/5
HIPASS J2100–71	21:00:13	–71:48:32	321.9	–35.5	2821	60	92	7.6	9.36	IC5069
HIPASS J2118–09	21:18:31	–09:01:16	42.3	–36.7	2574	59	79	16.9	9.72	IRAS21158–0914
HIPASS J2145–49	21:45:16	–49:02:00	348.5	–48.2	1600	71	115	27.1	9.44	ESO236-G039c
HIPASS J2217–45	22:17:23	–45:33:11	351.5	–54.4	3792	36	58	5.0	9.47	ESO289-G012

HIPASS Name	ATCA α, δ(J2000) [h,m,s]	[° ′ ″]	Offset from HIPASS [′]	PA [°]	ATCA-F_{HI} [Jy km s^{-1}]
HIPASS J0705–20	07:05:47	–20:59:30	0.5	100	13.5
HIPASS J1430–54	14:30:17	–54:36:10	0.3	315–345	7.3
HIPASS J1434–47	14:34:43	–47:13:30	1.9	—	2.7
HIPASS J1436–53	14:36:49	–53:34:27	0.3	100	26.4
HIPASS J1451–50	14:51:13	–50:12:47	1.7	300	23.7
HIPASS J1506–49	15:06:59	–49:25:39	0.9	160–170	25.9

Table 4: H I parameters from ATCA observations of six galaxies shown in Figure 13. The position angles (PA) were derived from the velocity field and may be affected by the elongated beam.


This figure "ryan-weber.fig4.jpg" is available in "jpg" format from:
http://arXiv.org/ps/astro-ph/0206447v1


This figure "ryan-weber.fig5.jpg" is available in "jpg" format from:
http://arXiv.org/ps/astro-ph/0206447v1


This figure "ryan-weber.fig6b.jpg" is available in "jpg" format from:
http://arXiv.org/ps/astro-ph/0206447v1


This figure "ryan-weber.fig7b.jpg" is available in "jpg" format from:
http://arXiv.org/ps/astro-ph/0206447v1


This figure "ryan-weber.fig8b.jpg" is available in "jpg" format from:
http://arXiv.org/ps/astro-ph/0206447v1


This figure "ryan-weber.fig9b.jpg" is available in "jpg" format from:
http://arXiv.org/ps/astro-ph/0206447v1


This figure "ryan-weber.fig13a.jpg" is available in "jpg" format from:
http://arXiv.org/ps/astro-ph/0206447v1


This figure "ryan-weber.fig13b.jpg" is available in "jpg" format from:
http://arXiv.org/ps/astro-ph/0206447v1


This figure "ryan-weber.fig13c.jpg" is available in "jpg" format from:
http://arXiv.org/ps/astro-ph/0206447v1


This figure "ryan-weber.fig13d.jpg" is available in "jpg" format from:
http://arXiv.org/ps/astro-ph/0206447v1


This figure "ryan-weber.fig13e.jpg" is available in "jpg" format from:
http://arXiv.org/ps/astro-ph/0206447v1


This figure "ryan-weber.fig13f.jpg" is available in "jpg" format from:
http://arXiv.org/ps/astro-ph/0206447v1


This figure "ryan-weber.fig14a.jpg" is available in "jpg" format from:
http://arXiv.org/ps/astro-ph/0206447v1

This figure "ryan-weber.fig14b.jpg" is available in "jpg" format from:

http://arXiv.org/ps/astro-ph/0206447v1